Collier, Dami A., De Marco, Anna, Ferreira, Isabella A.T.M., Meng, Bo, Datir, Rawlings, Walls, Alexandra C., Kemp S, Steven A., Bassi, Jessica, Pinto, Dora, Fregni, Chiara Silacci and others (2021) *Sensitivity of SARS-CoV-2 B.1.1.7 to mRNA vaccine-elicited antibodies.* Nature . ISSN 0028-0836.

Accelerated Article Preview

Sensitivity of SARS-CoV-2 B.1.1.7 to mRNA vaccine-elicited antibodies

Dami A. Collier, Anna De Marco, Isabella A.T.M. Ferreira, Bo Meng, Rawlings Datir, Alexandra C. Walls, Steven A. Kemp S, Jessica Bassi, Dora Pinto, Chiara Silacci Fregni, Siro Bianchi, M. Alejandra Tortorici, John Bowen, Katja Culap, Stefano Jaconi, Elisabetta Cameroni, Gyorgy Snell, Matteo S. Pizzuto, Alessandra Franzetti Pellanda, Christian Garzoni, Agostino Riva, Anne Elmer, Nathalie Kingston, Barbara Graves, Laura E. McCoy, Kenneth G. C. Smith, John R. Bradley, Nigel Temperton, L. Lourdes Ceron-Gutierrez, Gabriela Barcenas-Morales, William Harvey, Herbert W. Virgin, Antonio Lanzavecchia, Luca Piccoli, Rainer Doffinger, Mark Wills, David Veesler, Davide Corti, Ravindra K. Gupta,

This is a PDF file of a peer-reviewed paper that has been accepted for publication. Although unedited, the content has been subjected to preliminary formatting. Nature is providing this early version of the typeset paper as a service to our authors and readers. The text and figures will undergo copyediting and a proof review before the paper is published in its final form. Please note that during the production process errors may be discovered which could affect the content, and all legal disclaimers apply.

Article

Sensitivity of SARS-CoV-2 B.1.1.7 to mRNA vaccine-elicited antibodies

Dami A. Collier[1,2,3,18], Anna De Marco[4,18], Isabella A.T.M. Ferreira[1,2,18], Bo Meng[1,2,18], Rawlings Datir[1,2,3,18], Alexandra C. Walls[5], Steven A. Kemp S[1,2,3], Jessica Bassi[4], Dora Pinto[4], Chiara Silacci Fregni[4], Siro Bianchi[4], M. Alejandra Tortorici[5], John Bowen[5], Katja Culap[4], Stefano Jaconi[4], Elisabetta Cameroni[4], Gyorgy Snell[6], Matteo S. Pizzuto[4], Alessandra Franzetti Pellanda[7], Christian Garzoni[7], Agostino Riva[8], The CITIID-NIHR BioResource COVID-19 Collaboration*, Anne Elmer[9], Nathalie Kingston[10], Barbara Graves[10], Laura E. McCoy[3], Kenneth G. C. Smith[1,2], John R. Bradley[2,10], Nigel Temperton[11], L. Lourdes Ceron-Gutierrez[12], Gabriela Barcenas-Morales[12,13], The COVID-19 Genomics UK (COG-UK) consortium, William Harvey[14], Herbert W. Virgin[6], Antonio Lanzavecchia[4], Luca Piccoli[4], Rainer Doffinger[12,15], Mark Wills[2], David Veesler[5], Davide Corti[4,18 ✉] & Ravindra K. Gupta[1,2,15,16,17,18 ✉]

SARS-CoV-2 transmission is uncontrolled in many parts of the world, compounded in some areas by higher transmission potential of the B1.1.7 variant[1] now reported in 94 countries. It is unclear whether responses to SARS-CoV-2 vaccines based on the prototypic strain will be impacted by mutations found in B.1.1.7. Here we assessed immune responses following vaccination with mRNA-based vaccine BNT162b2[2]. We measured neutralising antibody responses following first and second immunisations using pseudoviruses expressing the wild-type Spike protein or the 8 amino acid mutations found in the B.1.1.7 spike protein. The vaccine sera exhibited a broad range of neutralising titres against the wild-type pseudoviruses that were modestly reduced against B.1.1.7 variant. This reduction was also evident in sera from some convalescent patients. Decreased B.1.1.7 neutralisation was also observed with monoclonal antibodies targeting the N-terminal domain (9 out of 10), the RBM (5 out of 31), but not in RBD neutralising mAbs binding outside the RBM. Introduction of the E484K mutation in a B.1.1.7 background to reflect a newly emergent Variant of Concern (VOC 202102/02) led to a more substantial loss of neutralising activity by vaccine-elicited antibodies and mAbs (19 out of 31) over that conferred by the B.1.1.7 mutations alone. E484K emergence on a B.1.1.7 background represents a threat to the vaccine BNT162b.

The mRNA BNT162b2 vaccine encodes the full-length trimerised S protein of SARS CoV-2[2], designed against the Wuhan-1 isolate. Concerns have been raised as to whether vaccines will be effective against newly emergent SARS-CoV-2 variants, such as B.1.1.7 (N501Y.V1). In clinical studies of BNT162b2, GMT rose after first dose with high levels of protection against infection and severe disease after the second dose[3].

Results

Thirty seven participants had received the first dose of the BNT162b2 mRNA vaccine three weeks prior to blood draw for serum and peripheral blood monoclear cells (PBMC) collection. Median age was 62 years

(IQR 47-84) and 35% were female. Twenty-one of these participants also had a blood draw 3 weeks after receiving the second dose of BNT162b2 mRNA vaccine. Serum IgG titres to Nucleocapsid (N) protein, S and the S receptor binding domain (RBD) were assayed (Extended Data Fig. 1a).

Using lentiviral pseudotyping we studied WT (wild type bearing D614G) and mutant B.1.1.7 S proteins (Fig. 1a) in order to measure neutralisation activity of vaccine-elicited sera. The vaccine sera exhibited a range of inhibitory dilutions giving 50% neutralisation (ID50) (Fig. 1b, c). The GMT against wild type (WT) following the second dose of vaccine was substantially higher than after the first dose (318 vs 77) (Fig. 1b–e). There was correlation between total Spike IgG titres and serum neutralisation titres (Extended Data Fig. 1b). A broad range of T cell responses

[1]Cambridge Institute of Therapeutic Immunology & Infectious Disease, Cambridge, UK. [2]Department of Medicine, University of Cambridge, Cambridge, UK. [3]Division of Infection and Immunity, University College London, London, UK. [4]Humabs Biomed SA, a subsidiary of Vir Biotechnology, Bellinzona, Switzerland. [5]Department of Biochemistry, University of Washington, Seattle, WA, USA. [6]Vir Biotechnology, San Francisco, CA, USA. [7]Clinic of Internal Medicine and Infectious Diseases, Clinica Luganese Moncucco, Lugano, Switzerland. [8]Division of Infectious Diseases, Luigi Sacco Hospital, University of Milan, Milan, Italy. [9]NIHR Cambridge Clinical Research Facility, Cambridge, UK. [10]NIHR Bioresource, Cambridge, UK. [11]University of Kent, Canturbury, UK. [12]Department of Clinical Biochemistry and Immunology, Addenbrooke's Hospital, Cambridge, UK. [13]Laboratorio de Inmunologia, S-Cuautitlán, UNAM, Mexico. [14]Institute of Biodiversity, University of Glasgow, Glasgow, UK. [15]Department of Haematology, University of Cambridge, Cambridge, UK. [16]University of KwaZulu Natal, Durban, South Africa. [17]Africa Health Research Institute, Durban, South Africa. [18]These authors contributed equally: Dami A. Collier, Anna De Marco, Isabella A. T. M. Ferreira, Bo Meng, Rawlings Datir, Davide Corti, Ravindra K. Gupta. *Lists of members and their affiliations appears in the Supplementary Information. ✉e-mail: dcorti@vir.bio; rkg20@cam.ac.uk

Article

was measured by IFN gamma FluoroSpot against SARS-CoV-2 peptides in vaccinees after first dose. These cellular responses did not correlate with serum neutralisation titres or IgG S antibody titres (Extended Data Fig. 1c-d).

We then generated mutated pseudoviruses carrying S protein with mutations N501Y, A570D and the H69/V70 deletion. We observed a small increase in the ability of sera from vaccinees and convalescent individuals to inhibit this triple mutant virus (Extended Data Fig. 2a, b, 2c). We next completed the full set of eight mutations in the S protein present in B.1.1.7 variant (Fig. 1a). 20/29 of those with neutralisation activity after first dose showed evidence of a reduction in B.1.1.7 neutralisation titres (Fig. 1b, c, Extended Data Fig. 3), with mean fold change of 3.2 (SD 5.7). Following the second dose, GMT was markedly increased compared with first dose titres, with mean fold change 1.9 (SD 0.9) (Fig. 1d, e). Amongst sera from 27 recovered individuals, the GMT at 50% neutralisation was 1334 for WT, significantly higher than post second dose vaccination (Fig. 1f, g). The fold change in ID50 for neutralisation of B.1.1.7 versus wild type (D614G) was 4.5 (Fig. 1f, g and Extended Data Fig. 4).

The E484K substitution (Fig. 2a) has been reported as an escape mutation for several monoclonal antibodies[4], and is present in the B.1.351 (501Y.V2) and P.1 (501Y.V3) lineages. As of 11th of February 2021, thirty B.1.1.7 sequences also had the E484K substitution (Fig. 2c). Phylogenetic analysis suggests that there have been multiple independent acquisitions, with one lineage appearing to expand over time, indicating active transmission (Fig. 2b). This has resulted in Public Health England naming this as a variant of concern (VOC 202102/02)[5]. We therefore generated pseudoviruses bearing B.1.1.7 spike mutations with or without additional E484K and tested these against sera obtained after first and second dose mRNA vaccine as well as against convalescent sera. Following second dose, we observed a significant loss of neutralising activity for the pseudovirus with B.1.1.7 spike mutations and E484K (Fig. 3d, e). The mean fold change for the E484K B.1.1.7 Spike was 6.7 compared to 1.9 for B.1.1.7, relative to WT (Fig. 3a–c, Extended Data Fig. 5). Similarly when we tested a panel of convalescent sera with a range of neutralisation titres (Fig. 1f, g, Extended Data Fig. 5), we observed additional loss of activity against the mutant B.1.1.7 spike with E484K, with fold change of 11.4 relative to WT (Fig. 3f, g, Extended Data Fig. 5).

B.1.1.7 monoclonal antibody sensitivity

We tested 60 mAbs isolated from 15 individuals that recovered from SARS-CoV-2 infection in early 2020 with an *in-vitro* pseudotyped neutralization assay against B.1.1.7 spike (Supplementary Table 1). 20 out of 60 (33.3%) mAbs showed a greater than 2-fold loss of neutralising activity of B.1.1.7 variant compared to WT SARS-CoV-2 (Fig. 4a, b and Extended Data Fig. 6). B.1.1.7 mutant virus fully escaped neutralization by 8 out of 10 NTD-targeting mAbs (80%) (Fig. 4c). Of the 31 RBM-targeting mAbs, 5 (16.1%) showed more than 100-fold decrease in B.1.1.7 neutralization, and additional 6 mAbs (19.4%) had a partial 2-to-10-fold reduction (Fig. 4d). Finally, all RBD-specific non-RBM-targeting mAbs tested fully retained B.1.1.7 neutralising activity (Fig. 4e).

To address the role of B.1.1.7 N501Y mutation in the neutralization escape from RBM-specific antibodies, we tested the binding of 50 RBD-specific mAbs to WT and N501Y mutant RBD by biolayer interferometry (Fig. 4f and Extended Data Fig. 7). The 5 RBM-specific mAbs that failed to neutralize B.1.1.7 variant (Fig. 4d) showed a complete loss of binding to N501Y RBD mutant (Fig. 4g, h), demonstrating a role for this mutation as an escape mechanism for certain RBM-targeting mAbs.

To assess the effect of E484K on this panel of mAbs we generated a SARS-CoV-2 pseudotype carrying the K417N, E484K and N501Y mutations (TM). The inclusion of the K417N substitution was prompted by the observation that substitutions at this position have been found in 5 sequences from recent viral isolates within the B.1.1.7 lineage (K417 to N, E or R). This is in keeping with convergent evolution of the virus towards

an RBD with N501Y, E484K and K417N/T as evidenced by B.1.351 and P.1 lineages. Importantly, mutations at K417 are reported to escape neutralization from mAbs, including the recently approved mAb LY-CoV016[4,6]. Out of the 60 mAbs tested, 20 (33.3%) showed >10 fold loss of neutralising activity of TM mutant compared to WT SARS-CoV-2 (Fig. 4a, b and Extended Data Fig. 6), and of these 19 are RBM-specific mAbs. As above, we addressed the role of E484K mutation in escape from RBM-specific antibodies, by testing the binding of 50 RBD-specific mAbs to WT and E484K mutant RBD by biolayer interferometry (Fig. 4f and Extended Data Fig. 8). Out of the 19 RBM-specific mAbs that showed reduced or loss of neutralization of TM mutant (Fig. 4d), 16 showed a complete or partial loss of binding to E484K RBD mutant (Fig. 4g, h), consistent with findings that E484K is an important viral escape mutation[7,8,39]. Three of these 16 mAbs also lost binding to an RBD carrying N501Y, indicating that a fraction of RBM antibodies are sensitive to both N501Y and E484K mutations. Similarly, 3 of the 19 mAbs that lost neutralization of TM mutant (S2D8, S2H7 and S2X128) were previously shown to lose binding and neutralization to the K417V mutant, and here shown to be sensitive to either N501Y or E484K mutations.

B.1.1.7 RBD binding to ACE2

Using biolayer interferometry, we found that ACE2 bound to the B.1.1.7 RBD with an affinity of 22 nM compared to 133 nM for the WT RBD (Extended Data Fig. 9), in agreement with our previous deep-mutational scanning measurements using dimeric ACE2[9]. Although ACE2 bound with comparable on-rates to both RBDs, the observed dissociation rate constant was slower for B.1.1.7 than for the WT RBD (Extended data Table 1). These findings might participate in the efficient ongoing transmission of this newly emergent SARS-CoV-2 lineage, and possibly reduced opportunity for antibody binding. To understand the impact of TM mutations (K417N, E484K and N501Y), we evaluated binding of ACE2 to the immobilized TM RBD. We determined an ACE2 binding affinity of 64 nM for the TM RBD, driven by a faster off-rate than observed for the B.1.1.7 RBD but slower than for the WT RBD. We propose that the K417N mutation is slightly detrimental to ACE2 binding explaining the intermediate affinity determined for the TM RBD compared to the B.1.17 and WT RBDs, likely as a result of disrupting the salt bridge formed with ACE2 residue D30.

Discussion

Serum neutralising activity is a correlate of protection for other respiratory viruses, including influenza[10] and respiratory syncytial virus where prohylaxis with monoclonal antibodies has been used in at-risk groups[11,12]. Neutralising antibody titres appeared to be highly correlated with vaccine protection against SARS-CoV-2 rechallenge in non-human primates[13,14].

This study reports on the neutralisation by sera collected after both the first and second doses of the BNT162b2 vaccine. The participants of this study were older adults, in line with the targeting of this age group in the initial rollout of the vaccination campaign in the UK. We demonstrated that a pseudovirus bearing S protein with the full set of mutations present in the B.1.1.7 variant did result in small reduction in neutralisation by sera from vaccinees that was more marked following the first dose than the second dose. This could be related to increased breadth/potency/concentration of antibodies following the boost dose. Other studies have reported a small reduction of neutralisation against the B.1.1.7 variant from individuals vaccinated with two doses of BNT162b2[15] and mRNA-1273[16]. The reduced neutralising activity observed with polyclonal antibodies elicited by mRNA vaccines observed in this study is further supported by the loss of neutralising activity observed with human mAbs directed to both RBD and, to a major extent, to NTD.

Multiple variants, including the 501Y.V2 and B.1.1.7 lineages, harbor multiple mutations as well as deletions in NTD, most of which

are located in a site of vulnerability that is targeted by all known NTD-specific neutralising antibodies[17,18]. The role of NTD-specific neutralising antibodies might be under-estimated, in part by the use of neutralization assays based on target cells over-expressing ACE2 receptors. NTD-specific mAbs were suggested to interfere with viral entry based on other accessory receptors, such as DC-SIGN and L-SIGN[19], and their neutralization potency was found to be dependent on different in vitro culture conditions[17]. The observation that 9 out of 10 NTD-specific neutralising antibodies failed to show a complete or near-complete loss of neutralising activity against B.1.1.7 indicates that this new variant may have also evolved to escape from this class of antibodies, that may have a yet unrecognized role in protective immunity. Taken together, the presence of multiple escape mutations in NTD is supportive of the hypothesis that this region of the spike, in addition to RBM, is also under immune pressure.

Worryingly, we have shown that there are multiple B.1.1.7 sequences in the UK bearing E484K with early evidence of transmission as well as independent aquisitions. We measured further reduction in neutralisation titres by vaccine sera when E484K was present alongside the B.1.1.7 S mutations. Wu and co-authors[16] have also shown that variants carrying the E484K mutation resulted in a 3-to-6 fold reduction in neutralization by sera from mRNA-1273 vaccinated individuals. Consistently, in this study we found that approximately 50% of the RBM mAbs tested lost neutralising activity against SARS-CoV-2 carrying E484K. E484K has been shown to impact neutralisation by monoclonal antibodies or convalescent sera, especially in combination with N501Y and K417N[7,20–23].

Vaccines are a key part of a long term strategy to bring SARS-CoV-2 transmission under control. Our data suggest that vaccine escape to current Spike directed vaccines designed against the Wuhan strain will be inevitable, particularly given that E484K is emerging independently and recurrently on a B.1.1.7 (501Y.V1) background, and given the rapid global spread of B.1.1.7. Other major variants with E484K such as 501Y.V2 and V3 are also spreading regionally. This should be mitigated by designing next generation vaccines with mutated S sequences and using alternative viral antigens.

Online content

Any methods, additional references, Nature Research reporting summaries, source data, extended data, supplementary information, acknowledgements, peer review information; details of author contributions and competing interests; and statements of data and code availability are available at https://doi.org/10.1038/s41586-021-03412-7.

1. Volz, E. et al. Transmission of SARS-CoV-2 Lineage B.1.1.7 in England: Insights from linking epidemiological and genetic data. medRxiv, 2020.2012.2030.20249034, https://doi.org/10.1101/2020.12.30.20249034 (2021).

2. Mulligan, M. J. et al. Phase I/II study of COVID-19 RNA vaccine BNT162b1 in adults. Nature 586, 589-593, https://doi.org/10.1038/s41586-020-2639-4 (2020).

3. Polack, F. P. et al. Safety and Efficacy of the BNT162b2 mRNA Covid-19 Vaccine. N Engl J Med 383, 2603-2615, https://doi.org/10.1056/NEJMoa2034577 (2020).

4. Wang, P. et al. Increased Resistance of SARS-CoV-2 Variants B.1.351 and B.1.1.7 to Antibody Neutralization. bioRxiv, https://doi.org/10.1101/2021.01.25.428137 (2021).

5. PHE. Public Health England statement on Variant of Concern and new Variant Under Investigation, <https://www.gov.uk/government/news/phe-statement-on-variant-of-concern-and-new-variant-under-investigation> (2021).

6. Thomson, E. C. et al. Circulating SARS-CoV-2 spike N439K variants maintain fitness while evading antibody-mediated immunity. Cell, https://doi.org/10.1016/j.cell.2021.01.037 (2021).

7. Greaney, A. J. et al. Comprehensive mapping of mutations to the SARS-CoV-2 receptor-binding domain that affect recognition by polyclonal human serum antibodies. Cell host & microbe, https://doi.org/10.1016/j.chom.2021.02.003 (2021).

8. Andreano, E. et al. SARS-CoV-2 escape in vitro from a highly neutralizing COVID-19 convalescent plasma. bioRxiv, 2020.2012.2028.424451, https://doi.org/10.1101/2020.12.28.424451 (2020).

9. Starr, T. N. et al. Deep Mutational Scanning of SARS-CoV-2 Receptor Binding Domain Reveals Constraints on Folding and ACE2 Binding. Cell 182, 1295-1310 e1220, https://doi.org/10.1016/j.cell.2020.08.012 (2020).

10. Verschoor, C. P. et al. Microneutralization assay titres correlate with protection against seasonal influenza H1N1 and H3N2 in children. PloS one 10, e0131531, https://doi.org/10.1371/journal.pone.0131531 (2015).

11. Kulkarni, P. S., Hurwitz, J. L., Simoes, E. A. F. & Piedra, P. A. Establishing Correlates of Protection for Vaccine Development: Considerations for the Respiratory Syncytial Virus Vaccine Field. Viral Immunol 31, 195-203, https://doi.org/10.1089/vim.2017.0147 (2018).

12. Goddard, N. L., Cooke, M. C., Gupta, R. K. & Nguyen-Van-Tam, J. S. Timing of monoclonal antibody for seasonal RSV prophylaxis in the United Kingdom. Epidemiol Infect 135, 159-162, https://doi.org/10.1017/S0950268806006601 (2007).

13. Mercado, N. B. et al. Single-shot Ad26 vaccine protects against SARS-CoV-2 in rhesus macaques. Nature 586, 583-588, https://doi.org/10.1038/s41586-020-2607-z (2020).

14. McMahan, K. et al. Correlates of protection against SARS-CoV-2 in rhesus macaques. Nature, https://doi.org/10.1038/s41586-020-03041-6 (2020).

15. Muik, A. et al. Neutralization of SARS-CoV-2 lineage B.1.1.7 pseudovirus by BNT162b2 vaccine-elicited human sera. Science, https://doi.org/10.1126/science.abg6105 (2021).

16. Wu, K. et al. mRNA-1273 vaccine induces neutralizing antibodies against spike mutants from global SARS-CoV-2 variants. bioRxiv, https://doi.org/10.1101/2021.01.25.427948 (2021).

17. McCallum, M. et al. N-terminal domain antigenic mapping reveals a site of vulnerability for SARS-CoV-2. bioRxiv, https://doi.org/10.1101/2021.01.14.426475 (2021).

18. Suryadevara, N. et al. Neutralizing and protective human monoclonal antibodies recognizing the N-terminal domain of the SARS-CoV-2 spike protein. bioRxiv, 2021.2001.2019.427324, https://doi.org/10.1101/2021.01.19.427324 (2021).

19. Soh, W. T. et al. The N-terminal domain of spike glycoprotein mediates SARS-CoV-2 infection by associating with L-SIGN and DC-SIGN. bioRxiv, 1-30, https://doi.org/10.1101/2020.11.05.369264 (2020).

20. Tegally, H. et al. Emergence and rapid spread of a new severe acute respiratory syndrome-related coronavirus 2 (SARS-CoV-2) lineage with multiple spike mutations in South Africa. medRxiv, 2020.2012.2021.20248640, https://doi.org/10.1101/2020.12.21.20248640 (2020).

21. Greaney, A. J. et al. Comprehensive mapping of mutations to the SARS-CoV-2 receptor-binding domain that affect recognition by polyclonal human serum antibodies. bioRxiv, 2020.2012.2031.425021, https://doi.org/10.1101/2020.12.31.425021 (2021).

22. Greaney, A. J. et al. Complete mapping of mutations to the SARS-CoV-2 spike receptor-binding domain that escape antibody recognition. Cell Host & Microbe (2020).

23. Weisblum, Y. et al. Escape from neutralizing antibodies by SARS-CoV-2 spike protein variants. Elife 9, e61312, https://doi.org/10.7554/eLife.61312 (2020).
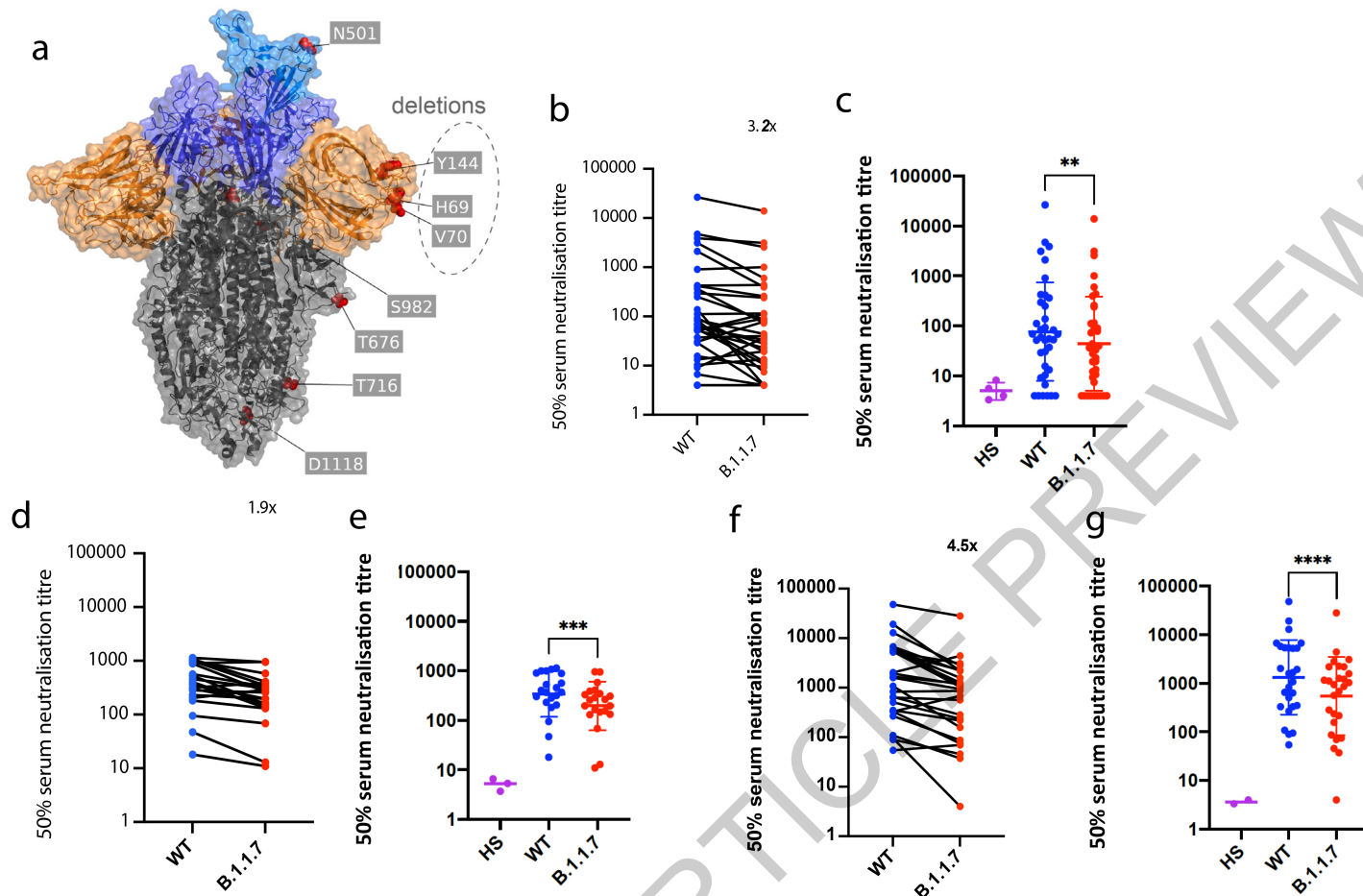
Fig. 1 | Neutralization by first and second dose mRNA vaccine sera against wild type and B.1.1.7 Spike mutant SARS-CoV-2 pseudotyped viruses. a, Spike in open conformation with a single erect RBD (PDB: 6ZGG) in trimer axis vertical view with the locations of mutated residues highlighted in red spheres and labelled on the monomer with erect RBD. Vaccine first dose (**b-c, n=37**), second dose (**d-e, n=21**) and convalescent sera, Conv. (**f-g, n=27**) against WT and B.1.1.7 Spike mutant with N501Y, A570D, ΔH69/V70, Δ144/145, P681H, T716I, S982A and D1118H. GMT with s.d presented of two independent experiments each with two technical repeats. Wilcoxon matched-pairs signed rank test. Two-tailed p-values ** <0.01, ***<0.001, **** <0.0001, ns not significant. No adjustment for multiple comparisons. HS – human AB serum control. Limit of detection for 50% neutralization set at 10. GMT: geometric mean titre for 50% neutralization.
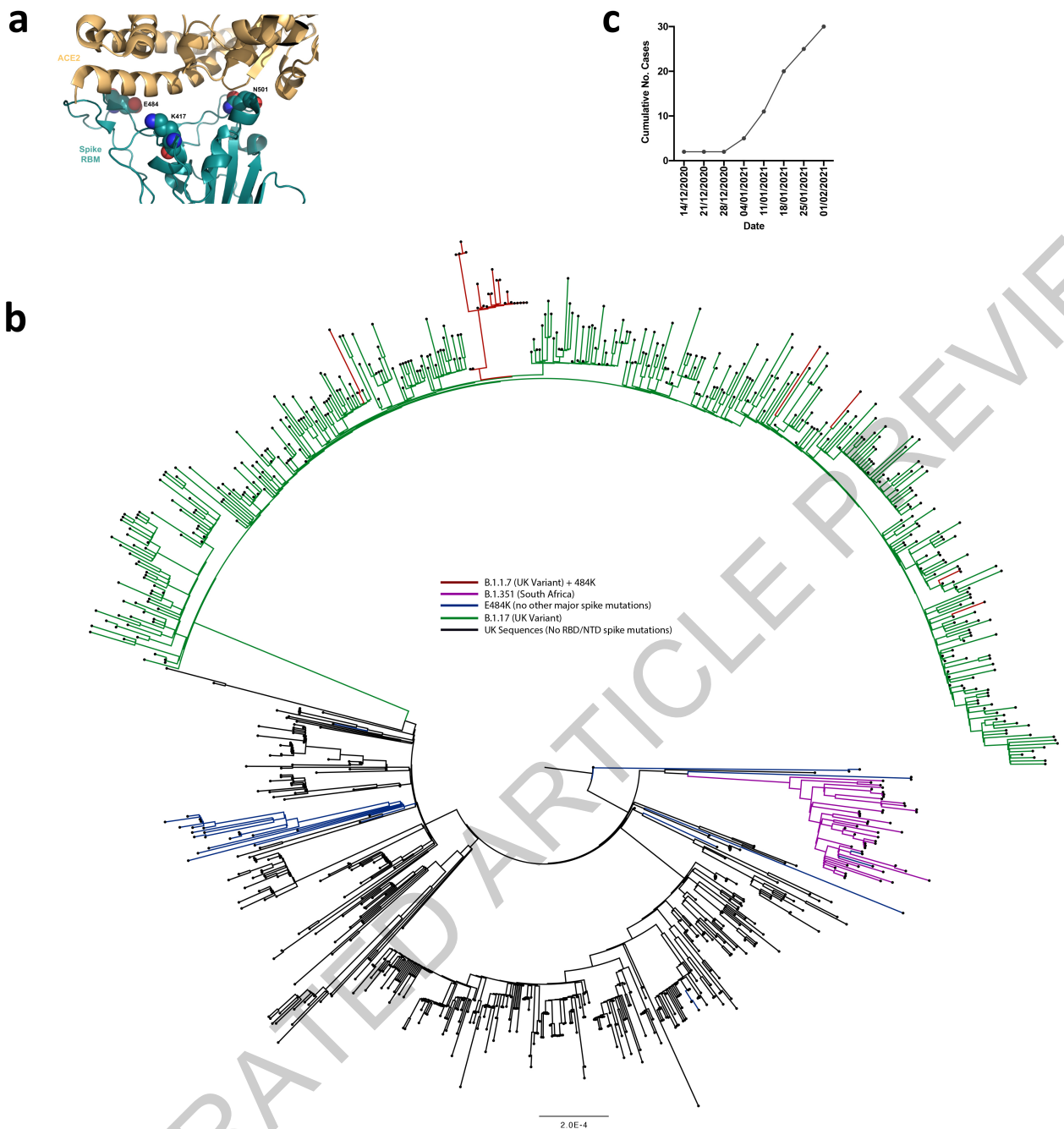
Fig. 2 | E484K appearing in background of B.1.1.7 with evidence of transmission. a. Representation of Spike RBM:ACE2 interface (PDB: 6M0J) with residues E484, N501 and K417 highlighted as spheres coloured by element **b.** Maximum likelihood phylogeny of a subset of sequences from the United Kingdom bearing the E484K mutation (green) and lineage B.1.1.7 (blue), with background sequences without RBD mutations in black. As of 11th Feb 2021, 30 sequences from the B.1.1.7 lineage (one cluster of 25 at top of phylogenetic tree) have acquired the E484K mutation (red). c. Sequence accumulation over time in GISAID for UK sequences with B.1.1.7 and E484K. RBD – receptor binding domain; NTD – N terminal domain.
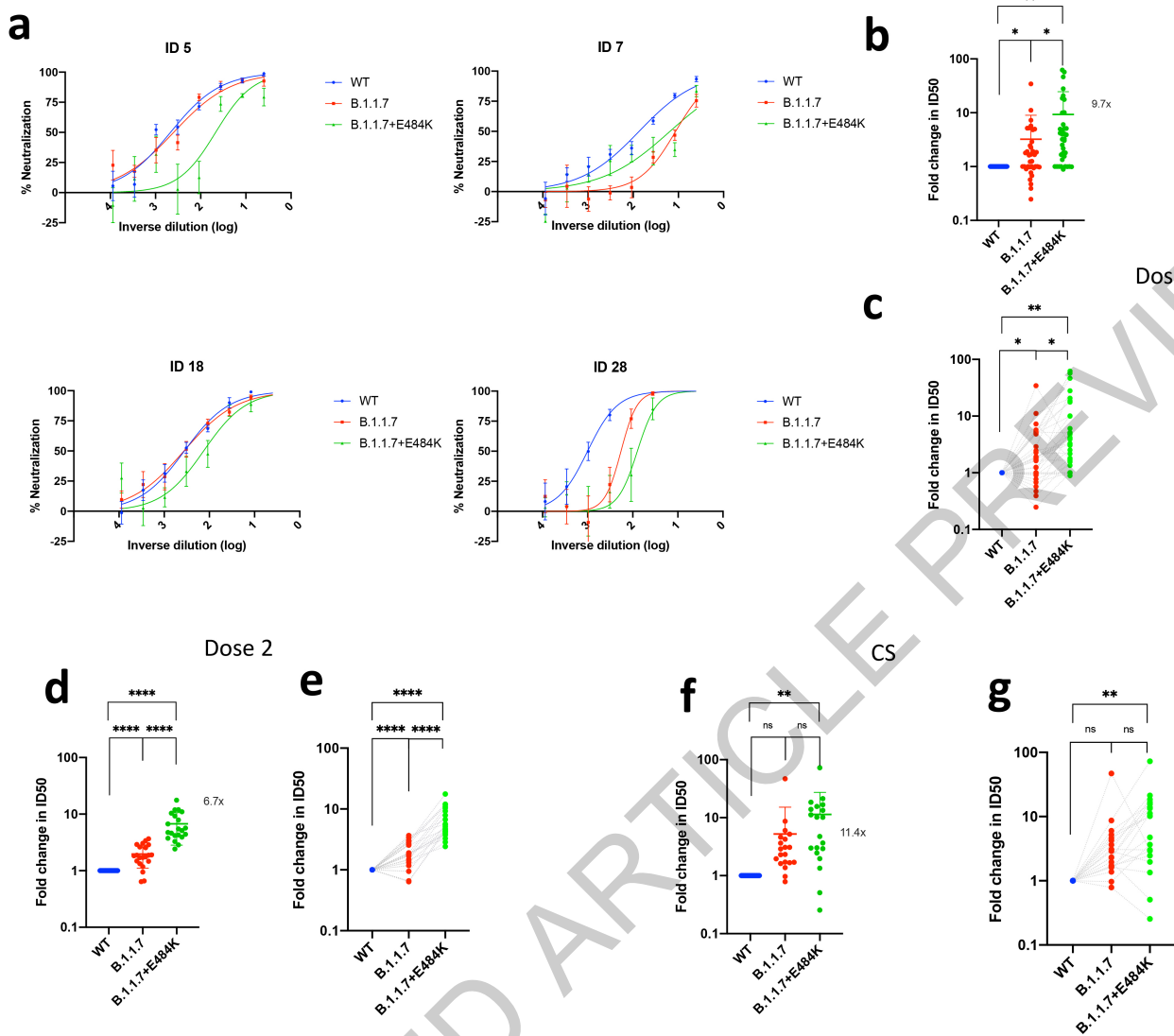
Fig. 3 | Neutralization potency of mRNA vaccine sera and convalescent sera (pre SARS-CoV-2 B.1.1.7) against pseudotyped virus bearing Spike mutations in the B1.1.7 lineage with and without E484K in the receptor binding domain (all In Spike D614G background). a, Example neutralization curves for vaccinated individuals. Data points represent mean of technical replicates with standard error and are representative of two independent experiments (**b-g**). 50% neutralisation titre for each virus against sera derived (**b,c**, n=37) following first vaccination (**d,e**, n=21) following second vaccination and (**f,g**, n=20) convalescent sera (CS) expressed as fold change relative to WT. Data points are mean fold change of technical replicates and are representative of two independent experiments. Central bar represents mean with outer bars representing s.d. Error bars for negative values are not shown. Paired T-test. Two-tailed p-values *<0.05, **<0.01, ****<0.0001; ns not significant. Limit of detection for 50% neutralization set at 10.
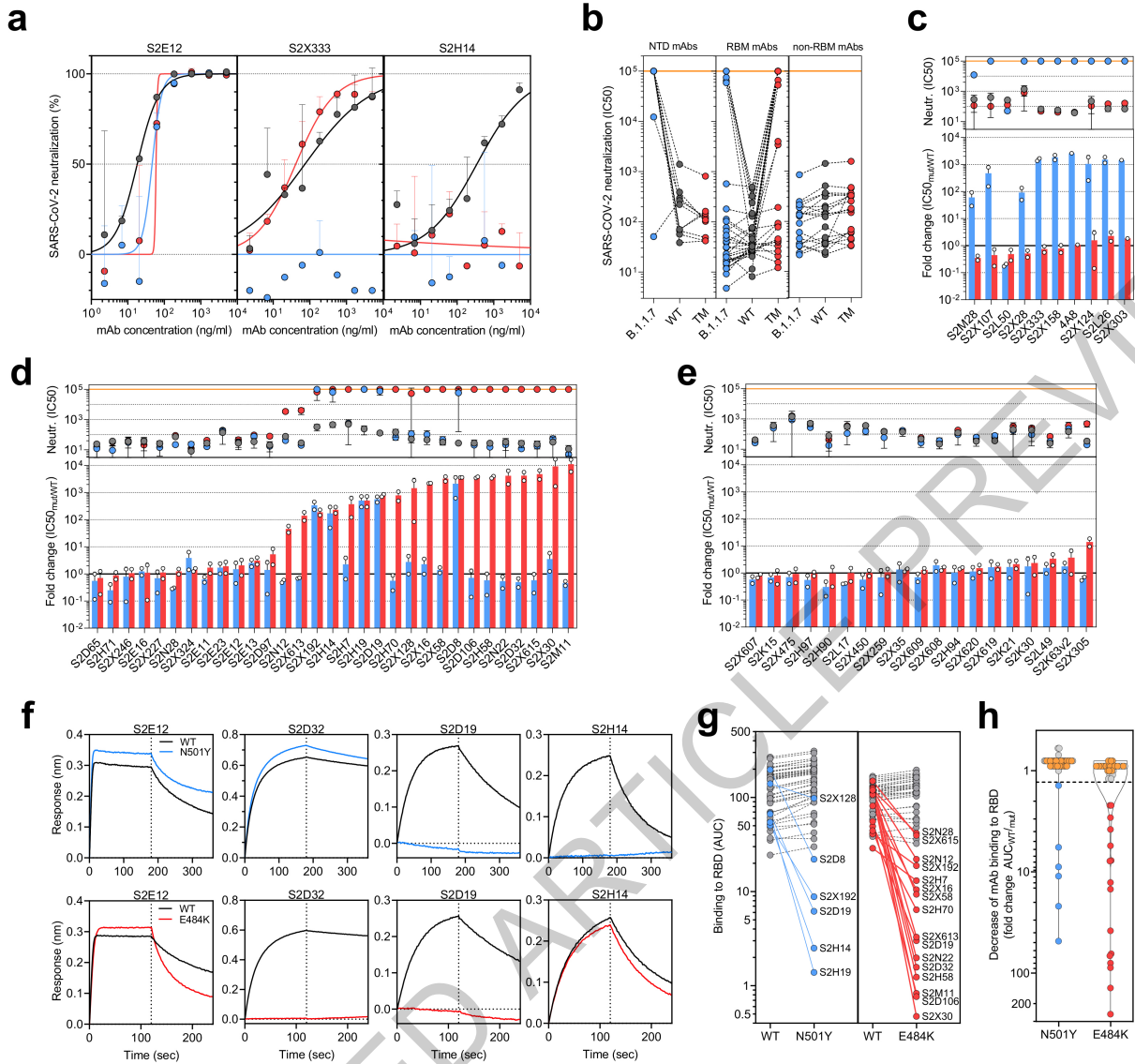
Fig. 4 | Neutralization and binding by a panel of NTD- and RBD-specific mAbs against WT, B.1.1.7 and RBD mutant SARS-CoV-2 viruses.
a, Neutralization of WT D614G (black), B.1.1.7 (blue) and a triple mutant (TM, carrying RBD mutations K417N/E484K/N501Y) (red) pseudotyped SARS-CoV-2-MLVs by 3 selected mAbs (S2E12, S2X333 and S2H14) from one representative experiment. Shown is the mean ± s.d. of 2 technical replicates. **b**, Neutralization of WT (D614G), B.1.1.7 and TM SARS-CoV-2-MLVs by 60 mAbs targeting NTD (n=10), RBM (n=31) and non-RBM sites in the RBD (n=19). Shown are the mean IC50 values (ng/ml) of n=2 independent experiments. **c-e**, Neutralization shown as mean IC50 values (upper panel) and mean fold change of B.1.1.7 (blue)

or TM (red) relative to WT (lower panel) of NTD (c), RBM (d) and non-RBM (e) mAbs. Upper panel shows mean IC50 values ± s.d from 2 independent experiments. Lower panel shows mean fold change ± s.d from 2 independent experiments. **f-h**, Kinetics of binding of mAbs to WT (black), N501Y (blue) and E484K (red) RBD as measured by bio-layer interferometry (BLI). Shown in (f) are the 4 RBM-targeting mAbs with no reduced binding to N501Y or E484K RBD. Area under the curve (AUC) (g) and AUC fold change (h) of 50 mAbs tested against WT, N501Y and E484K RBD. mAbs with a >1.3 AUC fold change shown in blue and red. mAbs: monoclonal antibodies. NTD: N-terminal domain.

Article

Methods

Participant recruitment and ethics

Participants who had received the first dose of vaccine and individuals with COVID-19 (Coronavirus Disease-19) were consented into the COVID-19 cohort of the NIHR Bioresource. The study was approved by the East of England – Cambridge Central Research Ethics Committee (17/EE/0025).

SARS-CoV-2 serology by multiplex particle-based flow cytometry (Luminex)

Recombinant SARS-CoV-2 N, S and RBD were covalently coupled to distinct carboxylated bead sets (Luminex; Netherlands) to form a 3-plex and analyzed as previously described (Xiong et al. 2020). Specific binding was reported as mean fluorescence intensities (MFI). Linear regression was used to explore the association between antibody response, T cell response and serum neutralisation in Stata 13. The Pearson correlation coefficient was reported.

Generation of S mutants

Amino acid substitutions were introduced into the D614G pCDNA_SARS-CoV-2_S plasmid as previously described[24] using the QuikChange Lightening Site-Directed Mutagenesis kit, following the manufacturer's instructions (Agilent Technologies, Inc., Santa Clara, CA). Sequences were checked by Sanger sequencing.

Preparation of B.1.1.7 or TM SARS-CoV-2 S glycoprotein-encoding-plasmid used to produce SARS-CoV-2-MLV based on overlap extension PCR. Briefly, a modification of the overlap extension PCR protocol[25] was used to introduce the nine mutations of the B.1.1.7 lineage or the three mutations in TM mutant in the SARS-CoV-2 S gene. In a first step, 9 DNA fragments with overlap sequences were amplified by PCR from a plasmid (phCMV1, Genlantis) encoding the full-length SARS-CoV-2 S gene (BetaCoV/Wuhan-Hu-1/2019, accession number mn908947). The mutations (del-69/70, del-144, N501Y, A570D, D614G, P681H, S982A, T716I and D1118H or K417N, E484K and N501Y) were introduced by amplification with primers with similar Tm. Deletion of the C-terminal 21 amino acids was introduced to increase surface expression of the recombinant S[26]. Next, 3 contiguous overlapping fragments were fused by a first overlap PCR (step 2) using the utmost external primers of each set, resulting in 3 larger fragments with overlapping sequences. A final overlap PCR (step 3) was performed on the 3 large fragments using the utmost external primers to amplify the full-length S gene and the flanking sequences including the restriction sites KpnI and NotI. This fragment was digested and cloned into the expression plasmid phCMV1. For all PCR reactions the Q5 Hot Start High fidelity DNA polymerase was used (New England Biolabs Inc.), according to the manufacturer's instructions and adapting the elongation time to the size of the amplicon. After each PCR step the amplified regions were separated on agarose gel and purified using Illustra GFX™ PCR DNA and Gel Band Purification Kit (Merck KGaA).

Pseudotype virus preparation

Viral vectors were prepared by transfection of 293T cells by using Fugene HD transfection reagent (Promega). 293T cells were transfected with a mixture of 11ul of Fugene HD, 1μg of pCDNAD19spike-HA, 1ug of p8.91 HIV-1 gag-pol expression vector[27,28], and 1.5μg of pCSFLW (expressing the firefly luciferase reporter gene with the HIV-1 packaging signal). Viral supernatant was collected at 48 and 72h after transfection, filtered through 0.45um filter and stored at -80˚C. The 50% tissue culture infectious dose ($TCID_{50}$) of SARS-CoV-2 pseudovirus was determined using Steady-Glo Luciferase assay system (Promega).

Serum/plasma pseudotype neutralization assay

Spike pseudotype assays have been shown to have similar characteristics as neutralisation testing using fully infectious wild type SARS-CoV-2[29]. Virus neutralisation assays were performed on 293T cell transiently transfected with ACE2 and TMPRSS2 using SARS-CoV-2 spike pseudotyped virus expressing luciferase[30]. Pseudotyped virus was incubated with serial dilution of heat inactivated human serum samples or sera from vaccinees in duplicate for 1h at 37˚C. Virus and cell only controls were also included. Then, freshly trypsinized 293T ACE2/TMPRSS2 expressing cells were added to each well. Following 48h incubation in a 5% CO_2 environment at 37 °C, luminescence was measured using the Steady-Glo or Bright-Glo Luciferase assay system (Promega). Neutralization was calculated relative to virus only controls. Dilution curves were presented as a mean neutralization with standard error of the mean (SEM). ID50 values were calculated in GraphPad Prism. The ID50 withing groups were summarised as a geometric mean titre and statistical comparison between groups were made with Wilxocon ranked sign test. In addition, the impact of the mutations on the neutralising effect of the sera were expressed as fold change (FC) of ID50 of the wild-type compared to mutant pseudotyped virus. Statistical difference in the mean FC between groups was determined using a 2-tailed t-test.

IFNγ FluoroSpot assays

Frozen PBMCs were rapidly thawed, and the freezing medium was diluted into 10ml of TexMACS media (Miltenyi Biotech), centrifuged and resuspended in 10ml of fresh media with 10U/ml DNase (Benzonase, Merck-Millipore via Sigma-Aldrich), PBMCs were incubated at 37 °C for 1h, followed by centrifugation and resuspension in fresh media supplemented with 5% Human AB serum (Sigma Aldrich) before being counted. PBMCs were stained with 2ul of each antibody: anti-CD3-fluorescein isothiocyanate (FITC), clone UCHT1; anti-CD4-phycoerythrin (PE), clone RPA-T4; anti-CD8a-peridinin-chlorophyll protein - cyanine 5.5 (PerCP Cy5.5), clone RPA-8a (all BioLegend, London, UK), LIVE/DEAD Fixable Far Red Dead Cell Stain Kit (Thermo Fisher Scientific). PBMC phenotyping was performed on the BD Accuri C6 flow cytometer. Data were analysed with FlowJo v10 (Becton Dickinson, Wokingham, UK). 1.5 to 2.5 x 105 PBMCs were incubated in pre-coated Fluorospot plates (Human IFNγ FLUOROSPOT (Mabtech AB, Nacka Strand, Sweden)) in triplicate with peptide mixes specific for Spike, Nucleocapsid and Membrane proteins of SARS-CoV-2 (final peptide concentration 1μg/ml/peptide, Miltenyi Biotech) and an unstimulated and positive control mix (containing anti-CD3 (Mabtech AB), Staphylococcus Enterotoxin B (SEB), Phytohaemagglutinin (PHA) (all Sigma Aldrich)) at 37 °C in a humidified CO2 atmosphere for 48 hours. The cells and medium were decanted from the plate and the assay developed following the manufacturer's instructions. Developed plates were read using an AID iSpot reader (Oxford Biosystems, Oxford, UK) and counted using AID EliSpot v7 software (Autoimmun Diagnostika GmbH, Strasberg, Germany). All data were then corrected for background cytokine production and expressed as spot forming units (SFU)/Million PBMC or CD3 T cells. The association between spike Tcell response, spike specific antibody response and serum neutralisation was deterimined using linear regression and the Pearson correlation coefficient between these variables were determined using Stata 13.

Ab discovery and recombinant expression

Human mAbs were isolated from plasma cells or memory B cells of SARS-CoV or SARS-CoV-2 immune donors, as previously described[31-34]. Recombinant antibodies were expressed in ExpiCHO cells at 37 °C and 8% CO2. Cells were transfected using ExpiFectamine. Transfected cells were supplemented 1 day after transfection with ExpiCHO Feed and ExpiFectamine CHO Enhancer. Cell culture supernatant was collected eight days after transfection and filtered through a 0.2 μm filter. Recombinant antibodies were affinity purified on an ÄKTA xpress FPLC device using 5 mL HiTrap™ MabSelect™ PrismA columns followed by buffer exchange to Histidine buffer (20 mM Histidine, 8% sucrose, pH 6) using HiPrep 26/10 desalting columns.

MAbs pseudovirus neutralization assay

MLV-based SARS-CoV-2 S-glycoprotein-pseudotyped viruses were prepared as previously described (Pinto et al., 2020). HEK293T/17cells were cotransfected with a WT, B.1.1.7 or TM SARS-CoV-2 spike glycoprotein-encoding-plasmid, an MLV Gag-Pol packaging construct and the MLV transfer vector encoding a luciferase reporter using X-tremeGENE HP transfection reagent (Roche) according to the manufacturer's instructions. Cells were cultured for 72 h at 37 °C with 5% CO_2 before harvesting the supernatant. VeroE6 stably expressing human TMPRSS2 were cultured in Dulbecco's Modified Eagle's Medium (DMEM) containing 10% fetal bovine serum (FBS), 1% penicillin–streptomycin (100 I.U. penicillin/mL, 100 µg/mL), 8 µg/mL puromycin and plated into 96-well plates for 16–24 h. Pseudovirus with serial dilution of mAbs was incubated for 1 h at 37 °C and then added to the wells after washing 2 times with DMEM. After 2–3 h DMEM containing 20% FBS and 2% penicillin–streptomycin was added to the cells. Following 48-72 h of infection, Bio-Glo (Promega) was added to the cells and incubated in the dark for 15 min before reading luminescence with Synergy H1 microplate reader (BioTek). Measurements were done in duplicate and relative luciferase units were converted to percent neutralization and plotted with a non-linear regression model to determine IC50 values using GraphPad PRISM software (version 9.0.0).

Antibody binding measurements using bio-layer interferometry (BLI)

MAbs (Supplementary Table 1) were diluted to 3 µg/ml in kinetic buffer (PBS supplemented with 0.01% BSA) and immobilized on Protein A Biosensors (FortéBio). Antibody-coated biosensors were incubated for 3 min with a solution containing 5 µg /ml of WT, N501Y or E484K SARS-CoV-2 RBD in kinetic buffer, followed by a 3-min dissociation step. Change in molecules bound to the biosensors caused a shift in the interference pattern that was recorded in real time using an Octet RED96 system (FortéBio). The binding response over time was used to calculate the area under the curve (AUC) using GraphPad PRISM software (version 9.0.0).

Production of SARS-CoV-2 and B.1.1.7 receptor binding domains and human ACE2

The SARS-CoV-2 RBD (BEI NR-52422) construct was synthesized by GenScript into CMVR with an N-terminal mu-phosphatase signal peptide and a C-terminal octa-histidine tag (GHHHHHHHH) and an avi tag. The boundaries of the construct are N-$_{328}$RFPN$_{331}$ and $_{528}$KKST$_{531}$-C[35]. The B.1.1.7 RBD gene was synthesized by GenScript into pCMVR with the same boundaries and construct details with a mutation at N501Y. These plasmids were transiently transfected into Expi293F cells using Expi293F expression medium (Life Technologies) at 37 °C 8% CO_2 rotating at 150 rpm. The cultures were transfected using PEI cultivated for 5 days. Supernatants were clarified by centrifugation (10 min at 4000xg) prior to loading onto a nickel-NTA column (GE). Purified protein was biotinylated overnight using BirA (Biotin ligase) prior to size exclusion chromatography (SEC) into phosphate buffered saline (PBS). Human ACE2-Fc (residues 1-615 with a C-terminal thrombin cleavage site and human Fc tag) were synthesized by Twist. Clarified supernatants were affinity purified using a Protein A column (GE LifeSciences) directly neutralized and buffer exchanged. The Fc tag was removed by thrombin cleavage in a reaction mixture containing 3 mg of recombinant ACE2-FC ectodomain and 10 µg of thrombin in 20 mM Tris-HCl pH8.0, 150 mM NaCl and 2.5 mM CaCl$_2$.The reaction mixture was incubated at 25 °C overnight and re-loaded on a Protein A column to remove uncleaved protein and the Fc tag. The cleaved protein was further purified by gel filtration using a Superdex 200 column 10/300 GL (GE Life Sciences) equilibrated in PBS.

Protein affinity measurement using bio-layer interferometry

Biotinylated RBD (WT, N501Y, or TM) were immobilized at 5 ng/uL in undiluted 10X Kinetics Buffer (Pall) to SA sensors until a load level of 1.1nm. A dilution series of either monomeric ACE2 or Fab in undiluted kinetics buffer starting at 1000-50nM was used for 300-600 seconds to determine protein-protein affinity. The data were baseline subtracted and the plots fitted using the Pall FortéBio/Sartorius analysis software (version 12.0). Data were plotted in Prism.

Phylogenetic analysis

All complete and low coverage excluded SARS-CoV-2 sequences were downloaded from the GISAID database (http://gisaid.org/)[36] on 11th February 2021. All sequences were realigned to the SARS-CoV-2 reference strain MN908947.3, using MAFFT v7.475 with automatic flavour selection and the --keeplength --addfragments options[37]. Sequences were then deduplicated. Major SARS-CoV-2 clade memberships were assigned to all sequences using the Nextclade server v0.12 (https://clades.nextstrain.org/).

Maximum likelihood phylogenetic trees were produced using the above curated dataset using IQ-TREE v2.1.2[38]. Evolutionary model selection for trees were inferred using ModelFinder[39] and trees were estimated using the GTR+F+I model with 1000 ultrafast bootstrap replicates[40]. All trees were visualised with Figtree v.1.4.4 (http://tree.bio.ed.ac.uk/software/figtree/) and manipulated and coloured with ggtree v2.2.4. Phylogenies were rooted on the SARS-CoV-2 reference sequence (MN908947.3) and nodes arranged in descending order.

Statistical analysis

Linear regression was used to explore the association between antibody response, T cell response and serum neutralisation in Stata 13. The Pearson correlation coefficient was reported.

Neutralisation data analysis

Neutralization was calculated relative to virus only controls. Dilution curves were presented as a mean neutralization with standard error of the mean (SEM). IC50 values were calculated in GraphPad Prism. The inhibitory dilution (ID50) within groups were summarised as a geometric mean titre and statistical comparison between groups were made with Wilxocon ranked sign test. In addition, the impact of the mutations on the neutralising effect of the sera were expressed as fold change of ID50 of the wild-type compared to mutant pseudotyped virus. Statistical difference in the mean FC between groups was determined using a 2-tailed t-test.

For antibody level

IFNγ FluoroSpot assay data analysis. The association between spike Tcell response, spike specific antibody response and serum neutralisation was determined using linear regression and the Pearson correlation coefficient between these variables were determined using Stata 13.

Reporting summary

Further information on research design is available in the Nature Research Reporting Summary linked to this paper.

Data availability

The neutralization and BLI data shown in Fig. 4 and Extended Data Figs. 6–8 can be found in Source Data for Fig. 4. All sequences are publicly available and were downloaded from http://gisaid.org. Deduplicated and subsampled data are freely available at https://github.com/StevenKemp/sequence_files/blob/main/vaccinepaper/with_background_subsampled_deduped_aligned_UKonly_484_vui.fasta.gz. Other data are available from the corresponding authors on request.

24. Gregson, J. *et al*. HIV-1 viral load is elevated in individuals with reverse transcriptase mutation M184V/I during virological failure of first line antiretroviral therapy and is associated with compensatory mutation L74I. *Journal of Infectious Diseases* (2019).

25. Forloni, M., Liu, A. Y. & Wajapeyee, N. Creating Insertions or Deletions Using Overlap Extension Polymerase Chain Reaction (PCR) Mutagenesis. *Cold Spring Harb Protoc* **2018**, https://doi.org/10.1101/pdb.prot097758 (2018).

26. Case, J. B. *et al*. Neutralizing Antibody and Soluble ACE2 Inhibition of a Replication-Competent VSV-SARS-CoV-2 and a Clinical Isolate of SARS-CoV-2. *Cell Host Microbe* **28**, 475-485 e475, https://doi.org/10.1016/j.chom.2020.06.021 (2020).

27. Naldini, L., Blomer, U., Gage, F. H., Trono, D. & Verma, I. M. Efficient transfer, integration, and sustained long-term expression of the transgene in adult rat brains injected with a lentiviral vector. *Proc Natl Acad Sci U S A* **93**, 11382-11388, https://doi.org/10.1073/pnas.93.21.11382 (1996).

28. Gupta, R. K. *et al*. Full length HIV-1 gag determines protease inhibitor susceptibility within in vitro assays. *AIDS* **24**, 1651 (2010).

29. Schmidt, F. *et al*. Measuring SARS-CoV-2 neutralizing antibody activity using pseudotyped and chimeric viruses. 2020.2006.2008.140871, https://doi.org/10.1101/2020.06.08.140871 %J bioRxiv (2020).

30. Mlcochova, P. *et al*. Combined point of care nucleic acid and antibody testing for SARS-CoV-2 following emergence of D614G Spike Variant. *Cell Rep Med*, **100099**, https://doi.org/10.1016/j.xcrm.2020.100099 (2020).

31. Corti, D. *et al*. A neutralizing antibody selected from plasma cells that binds to group 1 and group 2 influenza A hemagglutinins. *Science* **333**, 850-856, https://doi.org/10.1126/science.1205669 (2011).

32. Pinto, D. *et al*. Cross-neutralization of SARS-CoV-2 by a human monoclonal SARS-CoV antibody. *Nature* **583**, 290-295, https://doi.org/10.1038/s41586-020-2349-y (2020).

33. Tortorici, M. A. *et al*. Ultrapotent human antibodies protect against SARS-CoV-2 challenge via multiple mechanisms. *Science* **4**, eabe3354-3316, https://doi.org/10.1126/science.abe3354 (2020).

34. Piccoli, L. *et al*. Mapping neutralizing and immunodominant sites on the SARS-CoV-2 spike receptor-binding domain by structure-guided high-resolution serology. *Cell*, 1-55, https://doi.org/10.1016/j.cell.2020.09.037 (2020).

35. Walls, A. C. *et al*. Elicitation of Potent Neutralizing Antibody Responses by Designed Protein Nanoparticle Vaccines for SARS-CoV-2. *Cell* **183**, 1367-1382 e1317, https://doi.org/10.1016/j.cell.2020.10.043 (2020).

36. Shu, Y. & McCauley, J. GISAID: Global initiative on sharing all influenza data - from vision to reality. *Euro surveillance : bulletin Europeen sur les maladies transmissibles = European communicable disease bulletin* **22**, 30494, https://doi.org/10.2807/1560-7917.ES.2017.22.13.30494 (2017).

37. Katoh, K. & Standley, D. M. MAFFT multiple sequence alignment software version 7: improvements in performance and usability. *Mol Biol Evol* **30**, 772-780, https://doi.org/10.1093/molbev/mst010 (2013).

38. Minh, B. Q. *et al*. IQ-TREE 2: New Models and Efficient Methods for Phylogenetic Inference in the Genomic Era. *Mol Biol Evol* **37**, 1530-1534, https://doi.org/10.1093/molbev/msaa015 (2020).

39. Kalyaanamoorthy, S., Minh, B. Q., Wong, T. K. F., von Haeseler, A. & Jermiin, L. S. ModelFinder: fast model selection for accurate phylogenetic estimates. *Nat Methods* **14**, 587-589, https://doi.org/10.1038/nmeth.4285 (2017).

40. Minh, B. Q., Nguyen, M. A. & von Haeseler, A. Ultrafast approximation for phylogenetic bootstrap. *Mol Biol Evol* **30**, 1188-1195, https://doi.org/10.1093/molbev/mst024 (2013).

Author contributions Conceived study: D.C., RKG, DAC. Designed study and experiments: RKG, DAC, LEM, JB, MW, JT, LCG, GBM, RD, BG, NK, AE, M.P., D.V., L.P., A.D.M, J.B., D.C. Performed experiments: BM, DAC, NT, RD, IATMF, ACW, LCG, GBM. Interpreted data: RKG, DAC, BM, RD, IATMF, ACW, LEM, JB, KGCS, DV. ADM, JB and CSF carried out pseudovirus neutralization assays. DP produced pseudoviruses. MSP, LP, WH, DV and DC designed the experiments. MAT, JB, NS and SJ expressed and purified the proteins. KC, SJ and EC sequenced and expressed antibodies. EC and KC performed mutagenesis for mutant expression plasmids. ACW and S.B. performed binding assays. AR, AFP and CG contributed to donor's recruitment and sample collection related to mAbs isolation. HWV, GS, AL, DV, LP, DV and DC analyzed the data and prepared the manuscript with input from all authors.

Competing interests A.D.M., J.B., D.P., C.S.F., S.B., K.C., N.S., E.C., G.S., S.J., A.L., H.W.V., M.S.P., L.P. and D.C. are employees of Vir Biotechnology and may hold shares in Vir Biotechnology. H.W.V. is a founder of PierianDx and Casma Therapeutics. Neither company provided funding for this work or is performing related work. D.V. is a consultant for Vir Biotechnology Inc. The Veesler laboratory has received a sponsored research agreement from Vir Biotechnology Inc. The remaining authors declare that the research was conducted in the absence of any commercial or financial relationships that could be construed as a potential conflict of interest. RKG has received consulting fees from UMOVIS Lab, Gilead and ViiV.

Additional information
Supplementary information The online version contains supplementary material available at https://doi.org/10.1038/s41586-021-03412-7.
Correspondence and requests for materials should be addressed to D.C. or R.K.G.
**Peer review information** *Nature* thanks the anonymous reviewers for their contribution to the peer review of this work. Peer reviewer reports are available.
Reprints and permissions information is available at http://www.nature.com/reprints.

a
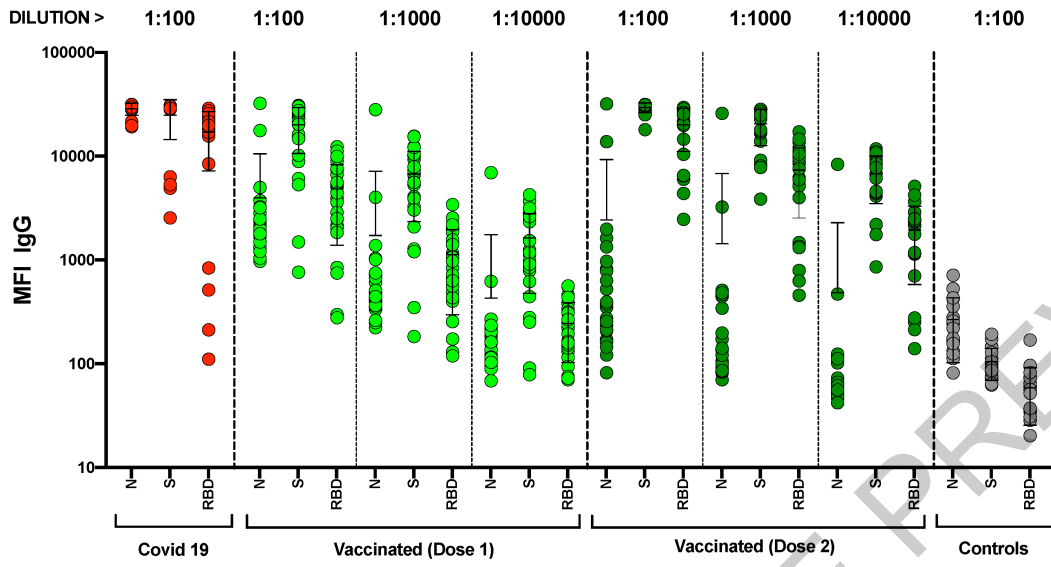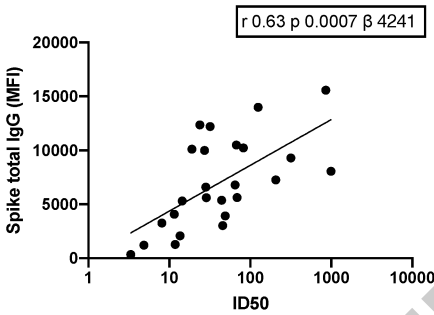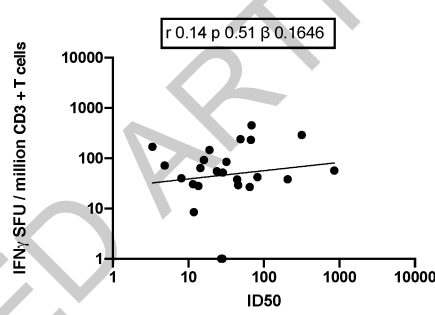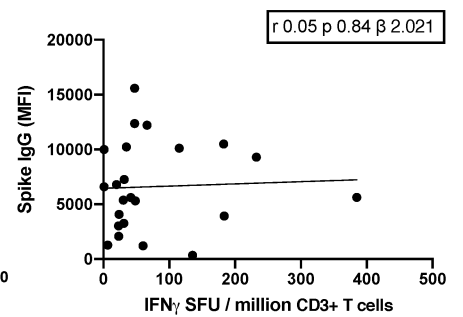
Extended Data Fig. 1 | Immune responses three weeks after first dose of Pfizer SARS-CoV-2 vaccine BNT162b2. a, N= 25, serum IgG responses against N protein, Spike and the Spike Receptor Binding Domain (RBD) from first vaccine participants (green), recovered COVID-19 cases (red), 3 convalescent plasma units and healthy controls (grey) as measured by a flow cytometry based Luminex assay. MFI, mean fluorescence intensity. Geometric mean titre (GMT with standard deviation (s.d) of two technical repeats presented. **b**, N=25, relationship between serum IgG responses as measured by flow cytometry and serum neutralisation ID50. **c**, N=24, relationship between serum neutralisation ID50 and T cell responses against SARS-CoV-2 by IFN gamma ELISpot. SFU: spot forming units. **d**, N=23, relationship between serum IgG responses and T cell responses. Simple linear regression is presented with Pearson correlation (r), P-value (p) and regression coefficient/slope (β).
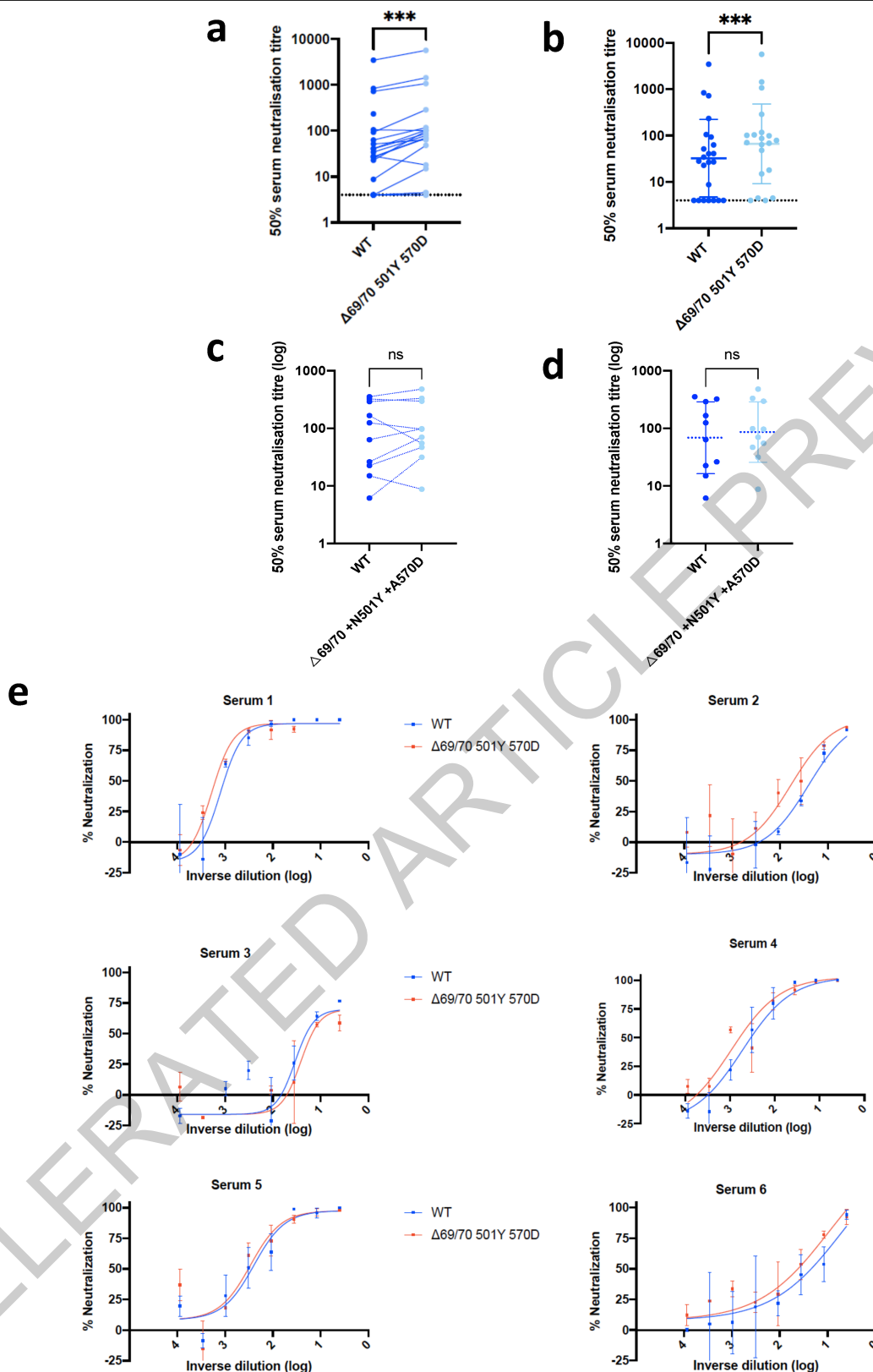
Extended Data Fig. 2 | Neutralization by first dose BNT162b2 vaccine and convalescent sera against wild type and mutant (N501Y, A570D, ΔH69/V70) SARS-CoV-2 pseudotyped viruses. (a-b) Vaccine sera dilution for 50% neutralization against WT and Spike mutant with N501Y, A570D, ΔH69/V70. Geometric mean titre (GMT) + s.d of two independent experiments with two technical repeats presented. Wilcoxon matched-pairs signed rank test. Two-tailed p-values ***<0.001, ns not significant. No adjustment for multiple comparisons. (c-d) Convalescent sera dilution for 50% neutralization against WT and Spike mutant with N501Y, A570D, ΔH69/V70. GMT + s.d of rep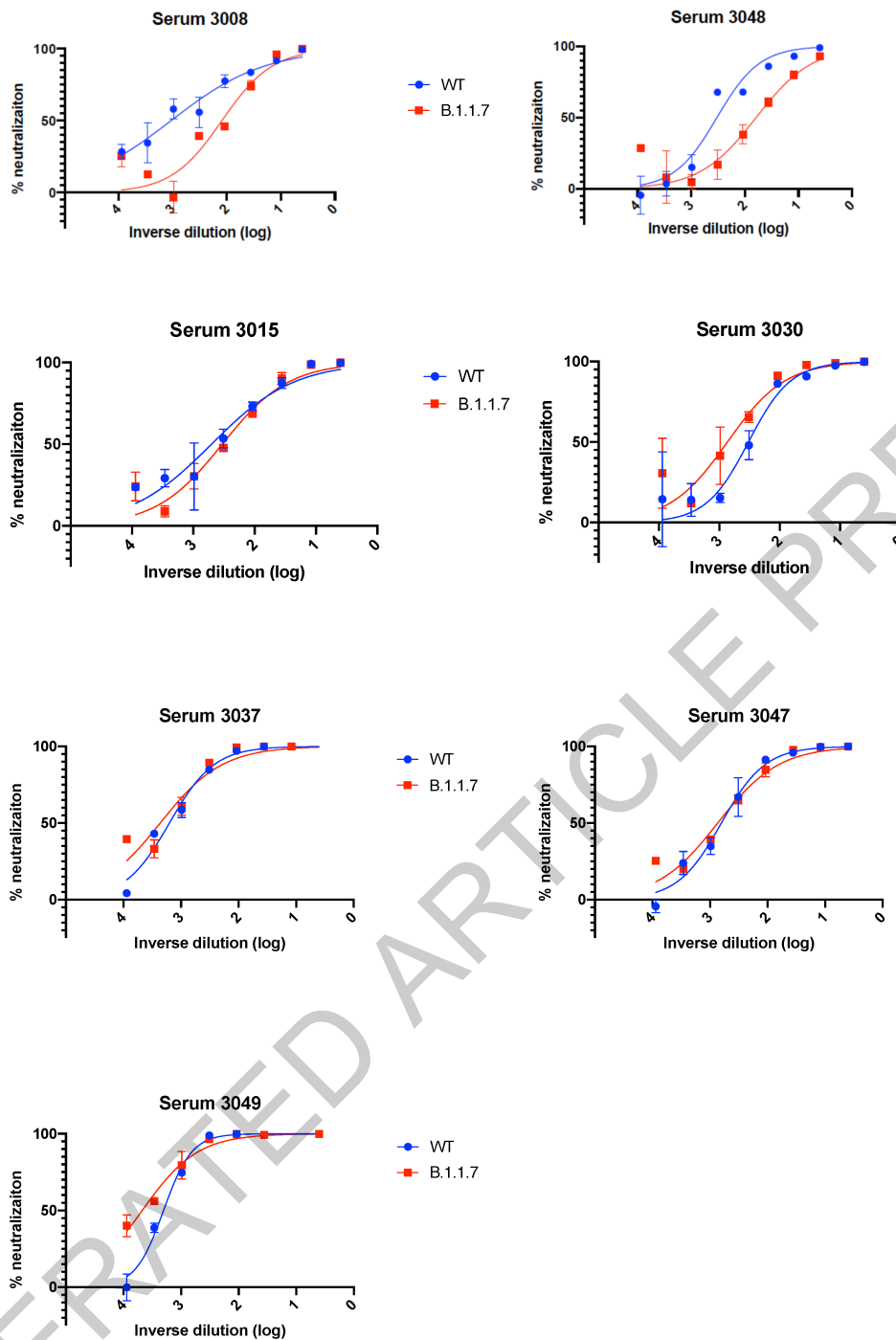resentative experiment with two technical repeats presented. **e**, Representative curves of convalescent serum $\log_{10}$ inverse dilution against % neutralization for WT v N501Y, A570D, ΔH69/V70. Where a curve is shifted to the right this indicates the virus is less sensitive to the neutralizing antibodies in the serum. Data are means of technical replicates and error bars represent standard error of the mean. Data are representative of 2 independent experiments. Limit of detection for 50% neutralization set at 10.
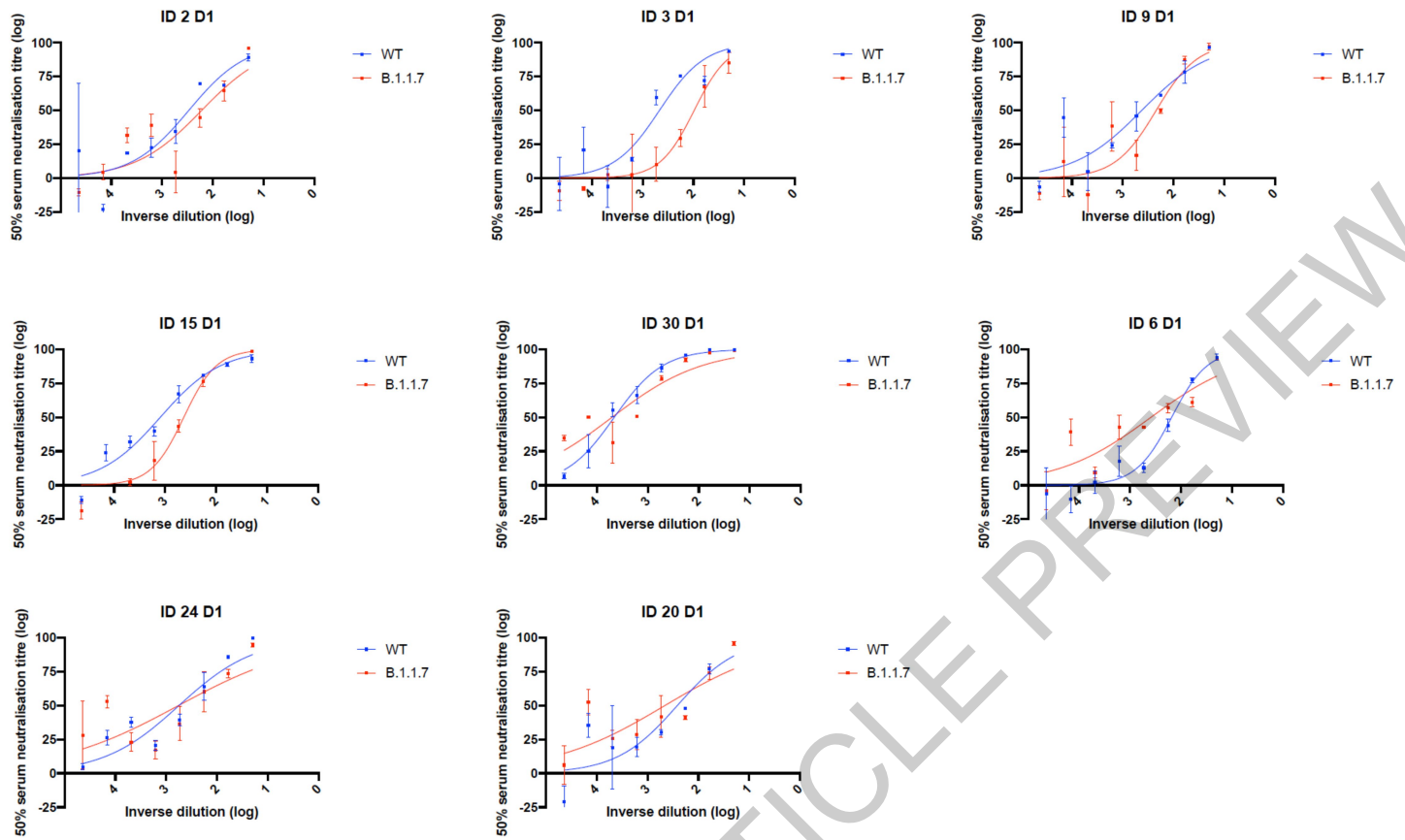
Extended Data Fig. 3 | Representative neutralization curves of BNT162b2 vaccine sera against pseudovirus virus bearing eight Spike mutations present in B.1.1.7 versus wild type (all In Spike D614G background). Indicated is serum $\log_{10}$ inverse dilution against % neutralization. Where a curve is shifted to the right this indicates the virus is less sensitive to the neutralizing antibodies in the serum. Data are for first dose of vaccine (D1). Data are representative of two independent experiments each with two technical replicates. Data points are means of technical replicates and error bars represent standard error of the mean. Limit of detection for 50% neutralization set at 10.

Extended Data Fig. 4 | Representative neutralization curves of convalescent sera against wild type and B.1.1.7 Spike mutant SARS-CoV-2 pseudoviruses. Indicated is serum $\log_{10}$ inverse dilution against % neutralization. Where a curve is shifted to the right this indicates the virus is less sensitive to the neutralizing antibodies in the serum. Data are representative of two independent experiments each with two technical replicates. Data points are means of technical replicates and error bars represent standard error of the mean. Limit of detection for 50% neutralization set at 10.
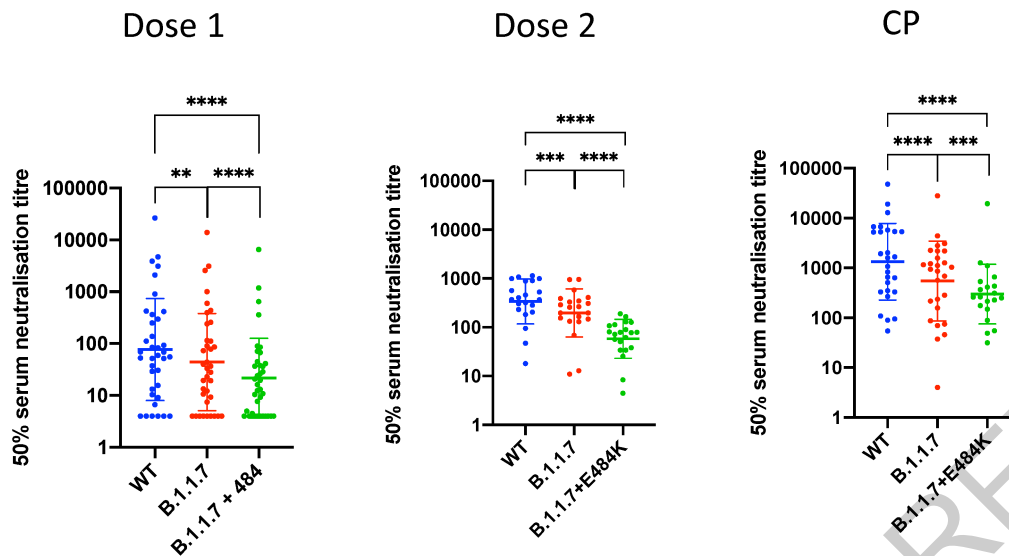
Extended Data Fig. 5 | Neutralisation potency of mRNA vaccine sera and convalescent sera (pre SARS-CoV-2 B.1.1.7) against pseudotyped virus bearing Spike mutations in the B.1.1.7 lineage with and without E484K in the receptor binding domain (all In Spike D614G background). Vaccine first dose (**a, n=37**), second dose (**b, n=21)** and convalescent sera, Conv. (**c=27**) against WT, B.1.1.7 Spike mutant with N501Y, A570D, ΔH69/V70, Δ144/145, P681H, T716I, S982A and D1118H and B.1.1.7 with E484K. GMT with s.d representative of two independent experiments each with two technical repeats are presented. Wilcoxon matched-pairs signed rank test p-values * <0.05, ** <0.01, ***<0.001, **** <0.0001, ns not significant. GMT: geometric mean titre for 50% neutralization.
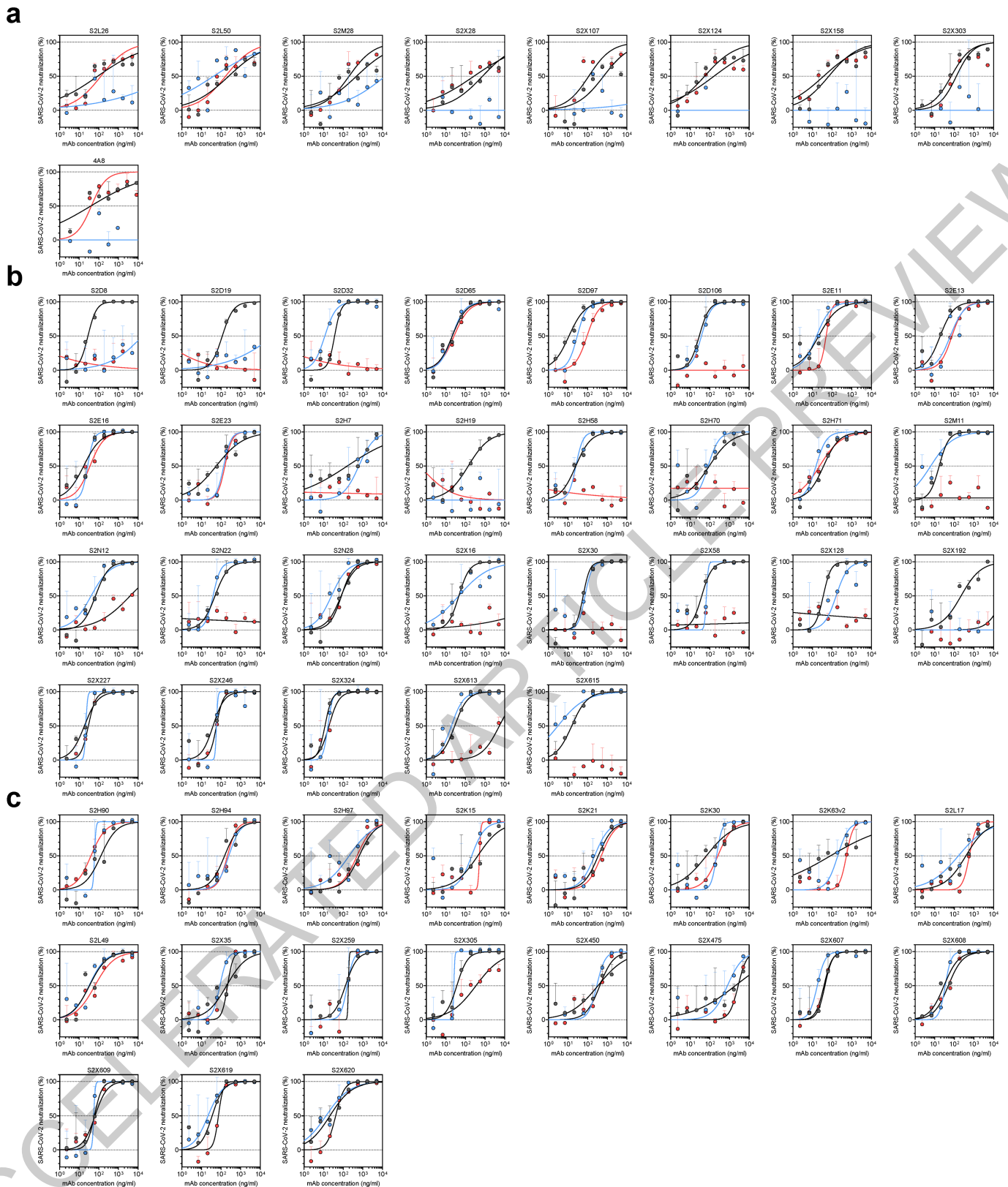
Extended Data Fig. 6 | Neutralisation of WT (D614G), B.1.1.7 and TM (N501Y, E484K, K417N) SARS-CoV-2 Spike pseudotyped virus by a panel of 57 monoclonal antibodies (mAbs). a-c, Neutralisation of WT (black), B.1.1.7 (blue) and TM (red) SARS-CoV-2-MLV by 9 NTD-targeting (a), 29 RBM-targeting (b) and 19 non-RBM-targeting (c) mAbs. Data from one representative experiment. Shown is the mean ± s.d. of 2 technical replicates.

a
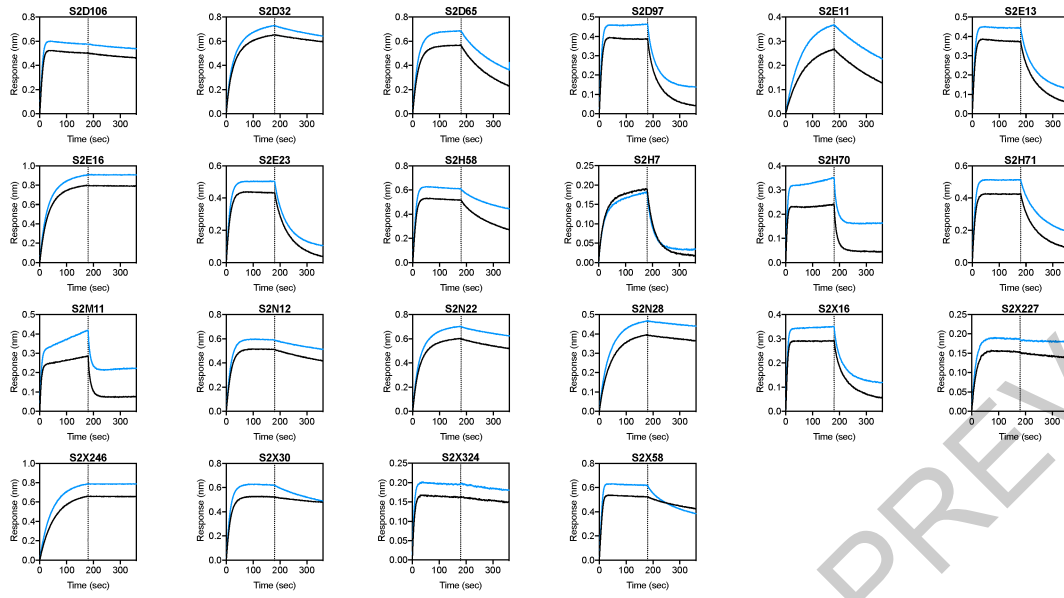
b
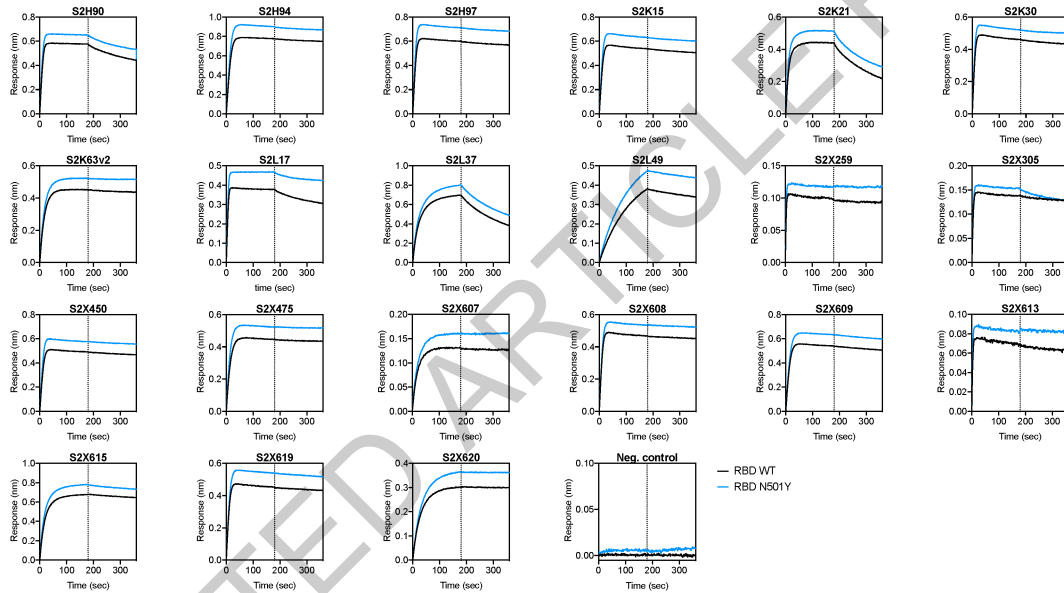
Extended Data Fig. 7 | Kinetics of binding to WT and N501Y SARS-CoV-2 RBD of 43 RBD-specific mAbs. a-b, Binding to WT (black) and N501Y (blue) RBD by 22 RBM-targeting (a) and 21 non-RBM-targeting (b) mAbs. An antibody of irrelevant specificity was included as negative control. mAbs: monoclonal antibodies.
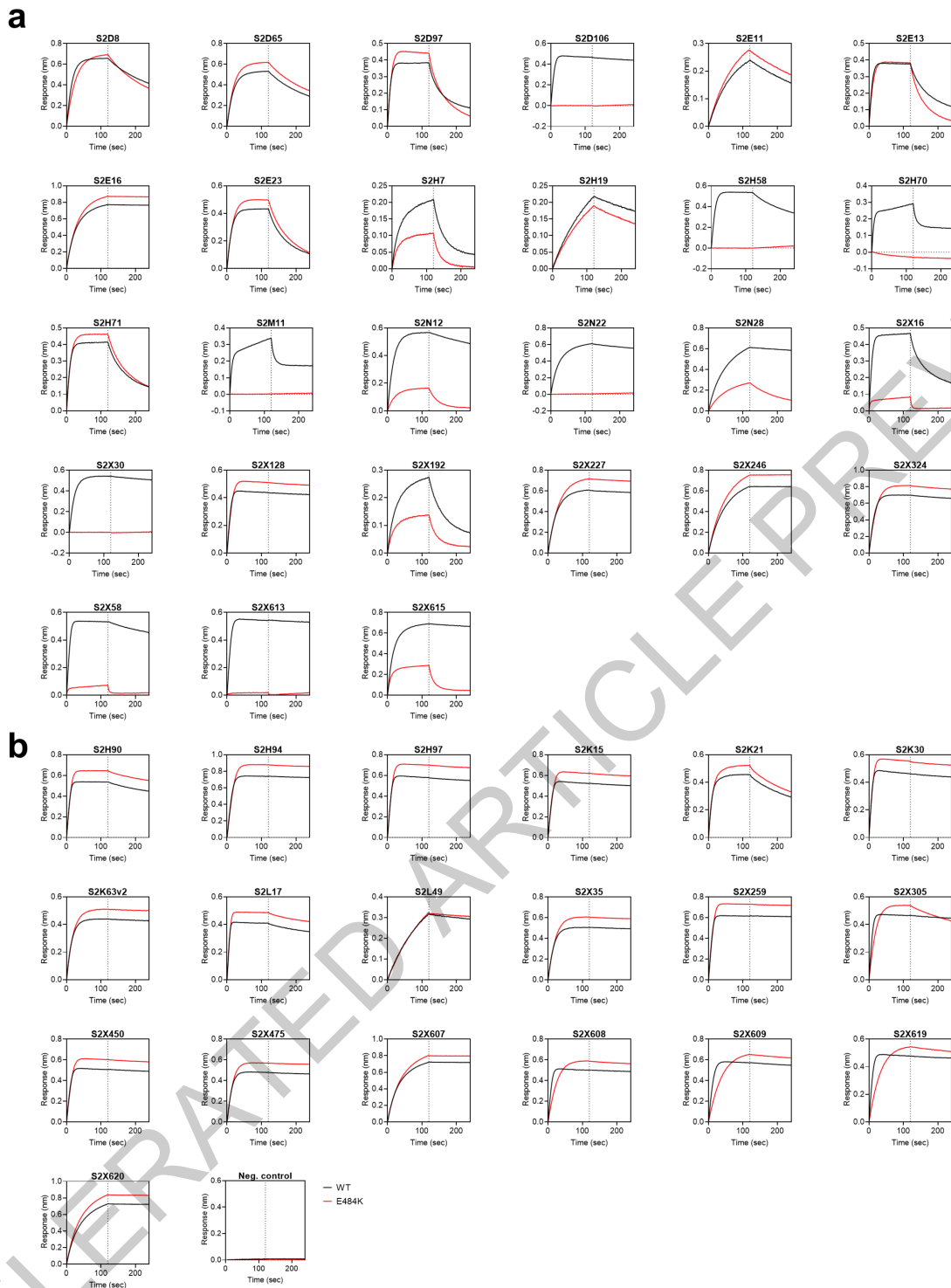
Extended Data Fig. 8 | Kinetics of binding to WT and E484K SARS-CoV-2 RBD of 46 RBD-specific mAbs. a-b, Binding to WT (black) and E484K (red) RBD by 27 RBM-targeting (a) and 19 non-RBM-targeting (b) mAbs. An antibody of irrelevant specificity was included as negative control. mAbs: monoclonal antibodies.
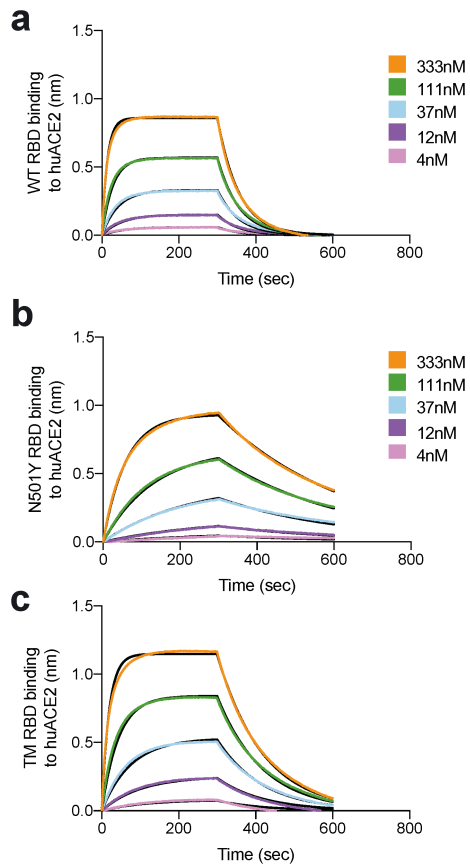
Extended Data Fig. 9 | Binding of human ACE2 to SARS-CoV-2 WT, N501Y, TM (N501Y, E484K, K417N) RBDs. a-b, BLI binding analysis of the human ACE2 ectodomain (residues 1-615) to immobilized SARS-CoV-2 WT RBD (a) and B.1.1.7 RBD (c). Black lines correspond to a global fit of the data using a 1:1 binding model. RBD: receptor binding domain.

Article

Extended data Table 1 | Kinetic analysis of human ACE2 binding to SARS-CoV-2 Wuhan-1, N501Y and N501Y/ E484K/ K417N (TM) RBDs by biolayer interferometry

		SARS-CoV-2 RBD WT	SARS-CoV-2 RBD N501Y	SARS-CoV-2 RBD TM
K_D (nM)		133	22	64
k_{on} ($M^{-1}.s^{-1}$)	hACE2	$1.3*10^5$	$1.4*10^5$	$1.3*10^5$
k_{off} (s^{-1})		$1.8*10^{-2}$	$3*10^{-3}$	$8.5*10^{-3}$

Values reported represent the global fit to the data shown in Extended Data Fig. 9.

nature research

Corresponding author(s): Ravindra K Gupta

Last updated by author(s): Feb 23, 2021

Reporting Summary

Nature Research wishes to improve the reproducibility of the work that we publish. This form provides structure for consistency and transparency in reporting. For further information on Nature Research policies, see our Editorial Policies and the Editorial Policy Checklist.

Statistics

For all statistical analyses, confirm that the following items are present in the figure legend, table legend, main text, or Methods section.

n/a	Confirmed	
☐	☒	The exact sample size (*n*) for each experimental group/condition, given as a discrete number and unit of measurement
☐	☒	A statement on whether measurements were taken from distinct samples or whether the same sample was measured repeatedly
☐	☒	The statistical test(s) used AND whether they are one- or two-sided *Only common tests should be described solely by name; describe more complex techniques in the Methods section.*
☒	☐	A description of all covariates tested
☒	☐	A description of any assumptions or corrections, such as tests of normality and adjustment for multiple comparisons
☐	☒	A full description of the statistical parameters including central tendency (e.g. means) or other basic estimates (e.g. regression coefficient) AND variation (e.g. standard deviation) or associated estimates of uncertainty (e.g. confidence intervals)
☐	☒	For null hypothesis testing, the test statistic (e.g. *F*, *t*, *r*) with confidence intervals, effect sizes, degrees of freedom and *P* value noted *Give P values as exact values whenever suitable.*
☒	☐	For Bayesian analysis, information on the choice of priors and Markov chain Monte Carlo settings
☒	☐	For hierarchical and complex designs, identification of the appropriate level for tests and full reporting of outcomes
☒	☐	Estimates of effect sizes (e.g. Cohen's *d*, Pearson's *r*), indicating how they were calculated

Our web collection on statistics for biologists contains articles on many of the points above.

Software and code

Policy information about availability of computer code

Data collection	Sequences were obtained from GISAID using the search parameters defined in the methods section. Monoclonal antibody binding data were collected with Octet RED96 system (FortéBio). Monoclonal antibody neutralization data (luminescence) were collected with Synergy H1 microplate reader (BioTek). Sera neutralising antibody data were read on a Glomax luminometer (Promega).
Data analysis	Graphad Prism v9 for statistical analyses and to produce figures. Monoclonal antibody binding data were analyzed by Pall FortéBio/Sartorius analysis software (version 12.0). Stata V13 for correlation analyses. PyMol v1.4 (Schodinger) to produce figures. Software versions and parameters used for all software are reported in full in the methods section.

For manuscripts utilizing custom algorithms or software that are central to the research but not yet described in published literature, software must be made available to editors and reviewers. We strongly encourage code deposition in a community repository (e.g. GitHub). See the Nature Research guidelines for submitting code & software for further information.

Data

Policy information about availability of data

All manuscripts must include a data availability statement. This statement should provide the following information, where applicable:

- Accession codes, unique identifiers, or web links for publicly available datasets
- A list of figures that have associated raw data
- A description of any restrictions on data availability

The data analysed during the current study are available freely online in the GISAID database (https//gisaid.org) though specific files may be requested from the corresponding author on reasonable request. Pymol structures were all obtained from PDB and are available using the accession numbers described in the methods.

Field-specific reporting

Please select the one below that is the best fit for your research. If you are not sure, read the appropriate sections before making your selection.

☒ Life sciences ☐ Behavioural & social sciences ☐ Ecological, evolutionary & environmental sciences

For a reference copy of the document with all sections, see nature.com/documents/nr-reporting-summary-flat.pdf

Life sciences study design

All studies must disclose on these points even when the disclosure is negative.

Sample size	n=37. No sample size calculation was performed. The sample size of this study is sufficient to obtain a relevant analysis.
Data exclusions	No exclusions.
Replication	We performed 2 independent experiments and presented representative data with technical replicates. All data were reproducible.
Randomization	This is not relevant to the study as it is not an interventional study.
Blinding	No blinding undertaken as this is not an interventional study.

Reporting for specific materials, systems and methods

We require information from authors about some types of materials, experimental systems and methods used in many studies. Here, indicate whether each material, system or method listed is relevant to your study. If you are not sure if a list item applies to your research, read the appropriate section before selecting a response.

Materials & experimental systems

n/a	Involved in the study
☐	☒ Antibodies
☐	☒ Eukaryotic cell lines
☒	☐ Palaeontology and archaeology
☒	☐ Animals and other organisms
☐	☒ Human research participants
☒	☐ Clinical data
☒	☐ Dual use research of concern

Methods

n/a	Involved in the study
☒	☐ ChIP-seq
☒	☐ Flow cytometry
☒	☐ MRI-based neuroimaging

Antibodies

Antibodies used	The source of monoclonal antibodies used in this study is described in Extended Data Table 1 and in the Method session.
Validation	The monoclonal antibodies were validated by binding and neutralization assays as described in the references of Extended Data Table 1.

Eukaryotic cell lines

Policy information about cell lines

Cell line source(s)	HEK 293T and ExpiCHO cells were used for transfection work to produce pseudoviruses and mAbs, respectively.
Authentication	No cell lines used were authenticated. No new cell lines were generated.
Mycoplasma contamination	All cell lines used were tested (by PCR) and were mycoplasma free.
Commonly misidentified lines (See ICLAC register)	No commonly misidentified lines were used in this study.

Human research participants

Population characteristics	Individuals receiving the Pfizer BNT162b2 mRNA vaccine were consented for the study. Median age was 62 years (IQR 47-84) and 35% were female.
Recruitment	Participants were consented into the COVID-19 cohort of the NIHR Bioresource. Consecutive individuals were enrolled without exclusion.
Ethics oversight	The study was approved by the East of England – Cambridge Central Research Ethics Committee (17/EE/0025).

Note that full information on the approval of the study protocol must also be provided in the manuscript.